Equivalent Circuits for Conventional and Extraordinary Reflection in Dipole Arrays

M. García-Vigueras, F. Mesa, F. Medina, R. Rodríguez-Berral, and J. L. Gómez-Tornero
Dept. Informat. & Communicat. Technologies, Technical University of Cartagena, 30202–Murcia, Spain
Grupo de Microondas, University of Seville, Av. Reina Mercedes s/n, 41012–Seville, Spain

***Abstract*— This presents an equivalent transmission-line circuit that accounts for the scattering of a TE polarized plane wave that impinges obliquely on a periodic array of metallic patches sandwiched in a dielectric slab. The proposed approach gives a very efficient reduced-order model of the electromagnetic phenomenon able to reproduce all the fine quantitative details of the reflection/transmission spectrum. Also, our model provides an easy theoretical frame to predict and/or understand all the qualitative behavior of the scattering when both oblique incidence and dielectric slabs are considered.**

***Index Terms*— Electromagnetic modeling, equivalent circuits, frequency selective surfaces.**

I. Introduction

Passive arrays of planar metallic patches (or apertures in a conducting screen) have recently attracted much interest in the field of engineering and physics. Considered as frequency selective surfaces (FSS), these periodic structures allow for the control of the reflection/transmission of electromagnetic waves. Thus, they have been used to design partially reflective surfaces [1], photonic/electromagnetic bandgap structures [2], [3], left-handed metamaterials [4], artificial magnetic conductors [5], etc. These artificially engineered materials have found numerous applications in different fields such as the synthesis of microwave/optical filters/resonators [3]–[5] and antenna enhancements [1], [6], [7]. For conventional FSS operation, the size and shape of periodic scatterers (patches/apertures) is tailored in order to control the characteristics of their first resonance [1], [8]–[12]. However, for scatterers of subwavelength size, a total reflection/transmission peak is also found before the onset of the first grating lobe. This latter resonance has been considered "extraordinary" since it is not directly related to the electrical length of the scatterers [13]–[15].

Although FSS are conceptually simple, their interaction with electromagnetic waves in stratified media may complicate considerably. Hence, FSS modeling and design have extensively been researched and several techniques have been proposed for the analysis of passive FSS under plane wave incidence in layered media [8]–[12], [14], [15]. Among these techniques, in this paper we will focus on the approach based on equivalent-circuit modeling [10]–[12], [14], [15]. In particular, we present an equivalent-circuit approach that makes no assumption on the electric length of the scatterers and that explicitly considers the dependence with the angle of incidence and with the characteristics of the dielectric slab. In order to compute the parameters of our equivalent circuit we need a reduced set of full-wave values, from which we can predict accurately high complicated spectra even beyond the appearance of grating lobes.

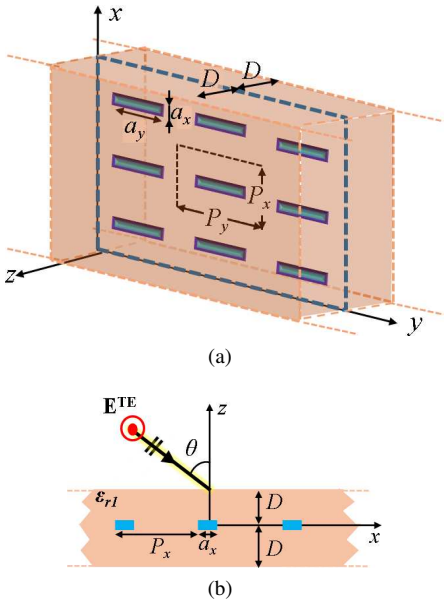

Fig. 1: (a) Array of conductors patches (metallic dipoles) sandwiched between identical dielectric slabs, (b) Plane wave excitation of the passive structure.

II. Theoretical Overview

FSS consisting of doubly periodic arrangements of metallic dipoles printed on a layered medium are extensively used nowadays for different applications [1], [4]–[7], [10], [12], [15]. In this paper we will focus our attention on the simpler case shown in Fig. 1a, where the periodic array of dipoles is assumed to be infinite in the xy plane and it is sandwiched between identical dielectric slabs. This structure was extensively studied in [8] because free-standing dipole-based FSS are unrealistic

978-1-61284-757-3/11/$26.00 C2011 IEEE

and, in general, undesirable. Moreover, dielectric slabs can be used to shape the reflection and transmission responses.

The passive structure of Fig. 1a is excited by an incident plane wave whose electric field is polarized along the y axis and its wavevector is contained in the yz plane (the direction of incidence is determined by θ); namely, the impinging wave is TE-polarized with its electric field parallel to the dipoles (see Fig. 1b). This polarization is typically considered in practical designs since it makes the incident waves be highly sensitive to the length of the metallic dipoles. Our goal in this work will be to find an appropriate but simple equivalent circuit that accounts for the wave scattering in this context of oblique incidence and presence of dielectric substrates. This equivalent circuit is not only expected to give the quantitative features of the scattering phenomenon but also to provide an adequate and simple theoretical frame able to explain and predict its qualitative behavior.

Due to periodicity, Floquet (space) harmonics are excited by the incident plane wave as it reaches the array [16]. These scattered waves can be either TE or TM polarized. The wavenumbers in the x and y axes associated with the space harmonics are given by

$$k_{x,m} = k_0 \sin\theta + \frac{2m\pi}{P_x} \quad \text{and} \quad k_{y,n} = \frac{2n\pi}{P_y} \qquad (1)$$

where m and n are integer numbers, and $k_0 = 2\pi f/c$ is the free-space wavenumber, with f being the frequency and c the free-space speed of light. Each excited space harmonic is defined by a pair of indexes, mn, and the following associated complex wavenumber along the z direction:

$$k_{z,mn}^{(\mathrm{d})} = \sqrt{k_0^2\varepsilon_r - k_{x,m}^2 - k_{y,n}^2}\,. \qquad (2)$$

Superscript (d) in this wavenumber stands for the presence of a dielectric medium with relative permittivity ε_r; when referring to free-space ($\varepsilon_r = 1$), the value of this superscript will be (0). For a lossless dielectric, the value of $k_{z,mn}^{(\mathrm{d})}$ can be either real or purely imaginary, thus defining propagative or evanescent waves, respectively. Although there exists an infinite number of space harmonics, in practice only a finite number of these is significant. The evanescent waves decay exponentially from the array whereas the propagative ones carry energy away from it. The incident plane wave in Fig. 1b corresponds to the dominant $mn = 00$ space harmonic. This wave propagates at any given frequency along the direction defined by θ (note from Eq. (2) that $k_{z,00}^{(0)/(\mathrm{d})}$ is always real). All other harmonics emanating from the array are evanescent below their cutoff frequency, $f_{\mathrm{c},mn}^{(\mathrm{d})}$; namely, the frequency at which it is satisfied that

$$\gamma_{mn}^2 = k_{x,m}^2 + k_{y,n}^2 - k_0^2\varepsilon_r = 0\,. \qquad (3)$$

Thus, the frequency $f_{\mathrm{c},mn}^{(\mathrm{d})}$ marks the onset of the corresponding mn-th harmonic in the dielectric medium. The value of this cutoff frequency is clearly lower than that in free space ($f_{\mathrm{c},mn}^{(\mathrm{d})} < f_{\mathrm{c},mn}^{(0)}$). This fact is very relevant in our case study since, at $f_{\mathrm{c},mn}^{(\mathrm{d})}$, each mn harmonic starts to propagate inside the dielectric slab but is still evanescent in free-space. It means that this harmonic is confined inside the slab and behaves as a trapped wave (see, for instance, [8, Ch. 5] for a detailed discussion). For $f > f_{\mathrm{c},mn}^{(0)}$, $k_{z,mn}^{(0)}$ is no longer imaginary and the mn harmonic starts to propagate away from the array creating a grating lobe in the direction of the wavevector $\mathbf{k}_{mn} = k_{x,m}\hat{\mathbf{x}} + k_{y,n}\hat{\mathbf{y}} + k_{z,mn}^{(0)}\hat{\mathbf{z}}$. The appearance of grating lobes is detrimental in practical FSS applications, and thus its operation regime is restricted to frequencies where only the dominant harmonic propagates along the free-space region.

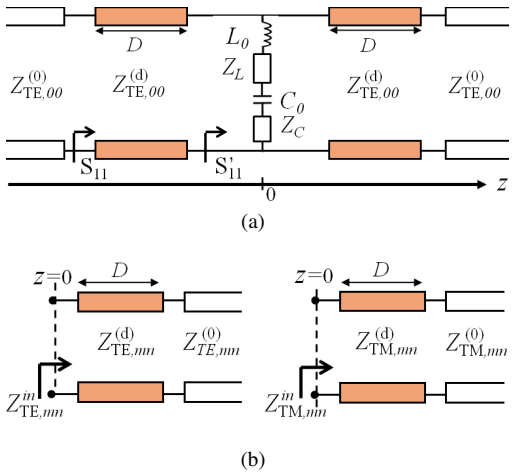

Fig. 2: Equivalent circuit for the scattering of an obliquely incident plane wave in the periodic array shown in Fig. 1a.

The transverse equivalent network shown in Fig. 2a is proposed to reproduce the scattering properties of the structure in Fig. 1a. Specifically, the propagation of the incident, reflected, and transmitted TE plane wave is modeled by the transmission lines placed at both sides of the discontinuity (namely, the FSS). The characteristic impedance of these lines is real and corresponds to

$$Z_{\mathrm{TE},00}^{(0)/(\mathrm{d})} = \omega\mu_0/k_{z,00}^{(0)/(\mathrm{d})}\,. \qquad (4)$$

The lumped elements in Fig. 2a model the excitation of all other mn harmonics in the discontinuity for a no-diffraction regime (below the appearance of grating lobes). These harmonic are evanescent waves with the following associated reactive characteristic impedances:

$$Z_{\mathrm{TE},mn}^{(\mathrm{d})} = \mathrm{j}\omega\mu_0/\gamma_{mn} \qquad (5)$$

$$Z_{\mathrm{TM},mn}^{(\mathrm{d})} = -\mathrm{j}\gamma_{mn}/(\omega\varepsilon_0\varepsilon_r)\,. \qquad (6)$$

In Fig. 2a, the inductive elements (L_0 and Z_L) account for TE harmonics whereas the capacitive components (C_0 and

978-1-61284-757-3/11/$26.00 C2011 IEEE

Z_C) account for the TM contribution. The impedances Z_L and Z_C, given by

$$Z_L = \sum_{h=1}^{N_{\rm TE}} A_h^{\rm TE} Z_{{\rm TE},h}^{\rm in} \quad ; \quad Z_C = \sum_{h=1}^{N_{\rm TM}} A_h^{\rm TM} Z_{{\rm TM},h}^{\rm in} \,, \qquad (7)$$

characterize the excitation of the significant $N_{\rm TE}$ and $N_{\rm TM}$ harmonics with lowest cutoff frequency, respectively. In these expressions each considered harmonic h is associated with a certain mn pair and $A_h^{\rm TE/TM}$ is a constant that accounts for the degree of excitation of each TE/TM h-th harmonic. The contribution of each TE/TM wave in (7) is proportional to the input impedance of its corresponding equivalent transmission line (shown in Fig. 2b), which can be expressed as

$$Z_{{\rm TE/TM},mn}^{\rm in} = Z_{{\rm TE/TM},mn}^{\rm (d)} \frac{Z_{{\rm TE/TM},mn}^{(0)} + {\rm j} Z_{{\rm TE/TM},mn}^{\rm (d)} \tan(k_{z,mn}^{\rm (d)} D)}{Z_{{\rm TE/TM},mn}^{\rm (d)} + {\rm j} Z_{{\rm TE/TM},mn}^{(0)} \tan(k_{z,mn}^{\rm (d)} D)} \,. \qquad (8)$$

The higher-order TE and TM harmonics that were not considered in (7) are highly evanescent waves responsible for the quasi-static behavior of the discontinuity. This quasi-static effect is accounted for by the frequency independent inductance, L_0, and capacitance, C_0, in Fig. 2a.

In our numerical computations, the values of $N_{\rm TE}$ and $N_{\rm TM}$ are taken respectively as one plus the number of TE and TM harmonics that are propagating inside the dielectric (trapped waves) below the onset of the first grating lobe. The values of the quasi-static components, L_0 and C_0, and the excitation coefficients, $A_h^{\rm TE/TM}$, can be computed from a few full-wave simulations of the reflection coefficient S_{11}. Taking into account Fig. 2, $S_{11}^{'}$ (which can easily be obtained from S_{11}) can be related to the lumped-element parameters in this figure in the following way:

$${\rm j}\omega L_0 + Z_L + \frac{1}{{\rm j}\omega C_0} + Z_C = \left(\frac{1 - S_{11}^{'}}{(1 + S_{11}^{'}) Z_{\rm TE,00}^{(0)}} - \frac{1}{Z_{\rm TE,00}^{\rm in}} \right)^{-1} . \qquad (9)$$

After writing the above equation for a number of frequencies (typically, two or three more than the number of unknowns) we can obtain a linear system of equations to compute the unknown constants $(L_0, C_0, A_h^{\rm TE/TM})$ via any appropriate solver (least squares, for instance). In next section, this equivalent transmission-line circuit will be applied in the modeling of particular designs.

III. Results

For simplicity, we first consider separately the problems of plane wave oblique incidence and presence of dielectric slabs. Full-wave results have been obtained (using the MoM-based technique proposed in [5]) for each studied case, showing excellent agreement with the equivalent circuit predictions. A square unit cell has been considered for all the analyzed cases, although rectangular shapes can equally be studied. Figure 3 shows the magnitude of the reflection coefficient ($|S_{11}|$) of a free standing FSS under oblique incidence. The results provided by our equivalent-circuit approach have been obtained by taking $D = 0$ mm (see Fig. 2a) and with $N_{\rm TE} = 2$ and $N_{\rm TM} = 1$ in (7). In Fig. 3 we observe null reflection (total transmission) at a certain frequency that decreases when increasing the angle of incidence. This effect is consistent with the total transmission expected by our equivalent circuit at the onset of the first TE-harmonic grating lobe. At this frequency, the impedance Z_L goes to infinity and behaves as an open circuit. The onset of the grating lobe then corresponds to the evanescent-to-propagative transition of the TE$_{-10}$ space harmonic, whose associated cutoff frequency can be expressed as

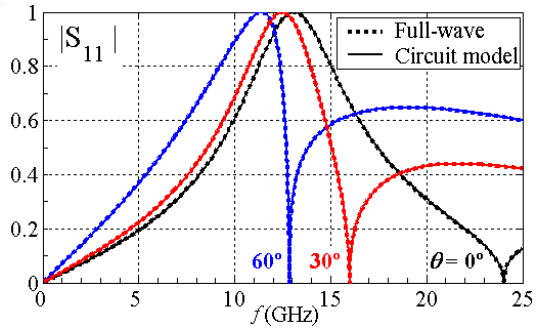

Fig. 3: Oblique plane wave incidence above a free-standing FSS with $P_x = P_y = 12.5\,$mm, $a_x = 2\,$mm, $a_y = 11\,$mm.

$$f_{\rm c,-10}^{\rm (d)} = \frac{c}{P_x \left(\sqrt{\varepsilon_r} + \sin\theta \right)} \qquad (10)$$

taking $\varepsilon_r = 1$ for free space. This expression predicts the onset of the first grating lobe at 24 GHz, 16 GHz, and 12.862 GHz for $\theta = 0^{\rm o}, 30^{\rm o}$ and $60^{\rm o}$ respectively, in total agreement with the values for which $|S_{11}| = 0$ in Fig. 3. The onset of the TM$_{-10}$ harmonic takes place at these same frequencies, where its associated impedance $Z_{\rm TM,-10}^{(0)}$ goes to zero, behaving as a short-circuit. Since all the components in the equivalent circuit are connected in series, the launch of TM harmonics does not produce any singularity in the reflection coefficient. In the no-diffraction regime, the standard FSS total reflection ($|S_{11}| = 1$) is produced at the resonance of the metallic dipoles (which, in this case, occurs approximately at 13 GHz, when $a_y \approx c/(2f)$). This phenomenon is also accurately predicted by the proposed resonant equivalent circuit.

978-1-61284-757-3/11/$26.00 C2011 IEEE

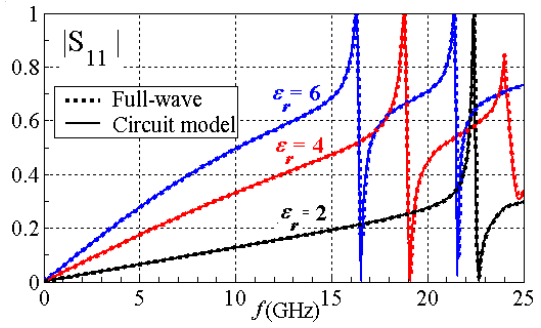

Fig. 4: Normal incident on a sandwiched FSS with $P_x = P_y = 12.5\,\text{mm}$, $a_x = 2\,\text{mm}$, $a_y = 3\,\text{mm}$ and $D = 0.5\,\text{mm}$.

The reflection under normal incidence experienced by a FSS sandwiched by identical dielectric slab is shown in Fig. 4. No anomaly is now observed at the onset of grating lobes in free space, since in this case $Z^{\text{in}}_{\text{TE/TM},-10}$ is finite at $f^{(0)}_{\text{c},-10}$. However, different trapped waves are launched inside the dielectric slab for $f^{(\text{d})}_{\text{c},-10} < f < f^{(0)}_{\text{c},-10}$. Due to the small electrical length (subwavelength) of the considered dipole ($a_y = 3$ mm), now the FSS does not show standard reflection but it does show the so-called extraordinary reflection. As the permittivity of the slab is increased, more peaks providing total reflection are generated below $f^{(0)}_{\text{c},-10}$, which correspond to new resonances caused by the frequency excursion of $Z^{\text{in}}_{\text{TE/TM},mn}$.

Finally, Fig.4 shows how the proposed equivalent-circuit approach enables the modeling of both conventional and extraordinary reflection ($a_y = 11\,\text{mm}$ and $a_y = 3\,\text{mm}$, respectively) when an oblique plane wave impinges on a sandwiched FSS.

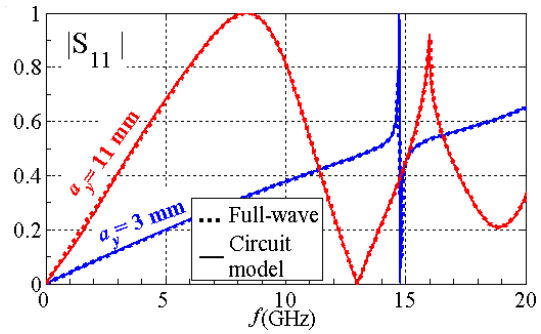

Fig. 5: Oblique ($\theta = 30^{\text{o}}$) plane wave incidence on a sandwiched FSS with $P_x = P_y = 12.5\,\text{mm}$, $a_x = 2\,\text{mm}$, $D = 0.5\,\text{mm}$ and $\varepsilon_r = 4$.

IV. Conclusions

A simple circuit model with very few adjustable parameters has been proposed to account for the reflection/transmission spectrum of sandwiched 2D arrays of metallic patches. These parameters are determined from full-wave MoM results at several arbitrary frequency points. A very good agreement is observed between our equivalent-circuit approach and numerical full-wave over the whole frequency band of interest.

Acknoledgments

This work has been supported by the Spanish Ministerio de Ciencia e Innovación and European Union FEDER funds (projects TEC2010-16948 and TEC2010-21520-C04-04), by Junta de Andalucía (project # TIC–253), and Regional Seneca project 08833/PI/08 (Regional Scholarship PMPDI-UPCT-2009).

References

[1] G. V. Trentini, "Partially reflective sheet arrays," *IRE Trans. Antennas Propag.*, vol. AP-4, pp. 666-671, 1956.

[2] E. Yablonovitch, T.J. Gmitter, and K.M. Leung, "Photonic band structure: the face-centered-cubic case employing nonspherical atoms," *Phys. Rev. Lett.*, vol.67, (17). pp. 2295-2298, 1991.

[3] D. Sievenpiper, L. Zhang, F. J. Broas, N. G. Alexopulos, and E. Yablonovitch, "High-impedance electromagnetic surfaces with a forbidden frequency band," *IEEE Trans. Microw. Theory Tech.*, vol. 47, no. 11, pp. 20592074, Nov. 1999.

[4] M Caiazzo, S. Maci, and N. Engheta, "A metamaterial surface for compact cavity resonators,"*IEEE Antennas Wireless Propag. Lett.*, vol. 3, pp. 261-264, 2004.

[5] G. Goussetis, A.P. Feresidis, and J.C. Vardaxoglou, "Tailoring the AMC and EBG characteristics of periodic metallic arrays printed on grounded dielectric substrate," *IEEE Trans. Antennas Propag.*, vol. 54, no. 1, pp. 82-89, Jan. 2006.

[6] Y. R. Lee, A. Charaya, D. S. Lockyer, and J. C. Vardaxoglou, "Dipole and tripole metallodielectric photonic bandgap (MPBG) structures for microwave filter and antenna applications," *Proc. Inst. Elect. Eng. Optoelectron.*, vol. 127, pp. 395400, Dec. 2000.

[7] A. P. Feresidis and J. C. Vardaxoglou, "High gain planar antenna using optimised partially reflective surfaces," *IEE Proc. Microw., Antennas and Propag.*, vol. 148, (6), pp. 345-350, Dec. 2001.

[8] B. Munk, *Frequency Selective Surfaces: Theory and Design,* Edt. John Wiley and Sons, 2000.

[9] John C. Vardaxoglou, *Frequency selective surfaces analysis and design,* Edt. Taunton Research Studies, 1997.

[10] S. Maci, M. Caiazzo, A. Cucini, and M. Casaletti, "A pole-zero matching method for EBG surfaces composed of a dipole FSS printed on a grounded dielectric slab," *IEEE Trans. Antennas Propag.*, vol. 53, no. 1, pp. 70-81, Jan. 2005.

[11] S. A. Tretyakov, *Analytical Modeling in Applied Electromagnetics,* Edt. Artech House, Norwood, MA, 2003

[12] M. García-Vigueras, J. L. Gómez-Tornero, G. Goussetis, J. S. Gómez- Diaz, and A. Álvarez-Melcón, "A modified pole-zero technique for the synthesis of waveguide leaky-wave antennas loaded with dipole-based FSS," *IEEE Trans. Antennas Propag.*, vol. 58, no. 6, pp. 1971-1979, June 2010.

[13] T. W. Ebbesen, H. J. Lezec, H. F. Ghaemi, T. Thio, and P. A. Wolff, "Extraordinary optical transmission through sub-wavelength hole arrays," *Nature*, vol. 391, pp. 667–669, Feb. 1998.

[14] F. Medina, F. Mesa, and R. Marqué s, "Extraordinary transmission through arrays of electrically small holes from a circuit theory perspective,"*IEEE Trans. Microw. Theory Tech.*, Vol. 56, No. 12, pp. 3108-3120, Dec. 2008.

[15] V. Lomakin and E. Michielssen, "Beam transmission through periodic subwavelength hole structures," *IEEE Trans. Antennas Propag.*, vol. 55, no. 6, pp. 1564-1581, June 2007.

[16] A. K. Bhattacharyya, *Phased Array Antennas Floquet Analysis, Synthesis, BFNs, and Active Array Systems,* Hoboken, NJ: Wiley, 2006.

978-1-61284-757-3/11/$26.00 C2011 IEEE